Effective magnetoelectric effect in multicoated circular fibrous multiferroic composites

Hsin-Yi Kuo and Ernian Pan

Citation: Journal of Applied Physics **109**, 104901 (2011); doi: 10.1063/1.3583580
View online: http://dx.doi.org/10.1063/1.3583580
View Table of Contents: http://scitation.aip.org/content/aip/journal/jap/109/10?ver=pdfcov
Published by the AIP Publishing

Effective magnetoelectric effect in multicoated circular fibrous multiferroic composites

Hsin-Yi Kuo[1,a)] and Ernian Pan[2]
[1]*Department of Civil Engineering, National Chiao Tung University, Hsinchu 300, Taiwan, Republic of China*
[2]*School of Mechanical Engineering, Zhengzhou University, Henan, People's Republic of China and Department of Civil Engineering, University of Akron, Ohio 44325, USA*

(Received 25 January 2011; accepted 26 March 2011; published online 16 May 2011)

Rayleigh's formalism is generalized for the evaluation of the effective material properties in multicoated circular fibrous multiferroic composites. The derived solution is applied to the special three-phase composite in which coated fibers are embedded in a matrix. For composites made of piezoelectric ($BaTiO_3$) and piezomagnetic ($CoFe_2O_4$ or Terfenol-D) phases, we find that the magnetoelectric effect in the composite made of $CoFe_2O_4$ coated $BaTiO_3$ in matrix Terfenol-D is five times larger than that in the composite made of $BaTiO_3$ coated Terfenol-D in matrix $CoFe_2O_4$. Furthermore, in each case, with appropriate coating to the circular fiber, the magnetoelectric effect in the coated composites can be enhanced by more than one order of magnitude as compared to the corresponding noncoating composite. © *2011 American Institute of Physics*. [doi:10.1063/1.3583580]

I. INTRODUCTION

This work is concerned with the magnetoelectric (ME) effect of a periodic array of multicoated circular fibrous piezoelectric-piezomagnetic composites. ME materials, which simultaneously show two or more types of ferroelectric, magnetic, or elastic orderings, have been the focus of research due to the varieties of their microstructural phenomena and macroscopic properties. These make them promising for a wide range of applications, such as magnetic field sensors, electrically controlled microwave phase shifters, four-state memories, etc.[1,2] However, this coupling is weak in single-phase materials, and is often observed only at very low temperatures. For instance, Cr_2O_3 has a ME voltage coefficient of 0.02 V/cmOe below the antiferromagetic Néel temperature of 307 K.[3] This is insufficient for practical applications and thus has motivated the study of composites of piezoelectric and piezomagnetic media, as reviewed recently by Spaldin and Fiebig,[4] Eerenstein *et al.*,[1] Nan *et al.*,[2] and Srinivasan.[5] The "product property" causes the ME effect in multiferroic composites: an applied electric field creates a strain in the piezoelectric material, which in turn creates a strain in the piezomagnetic material, resulting in a magnetic polarization.

A number of micromechanical models for two phase composites were proposed to predict the effective moduli of multiferroic composites. Among them, Nan[6] and Huang and Kuo[7] used the Green's function approach to study a fibrous composite consisting of $BaTiO_3$ and $CoFe_2O_4$. Benveniste[8] derived an exact expression for the effective magnetoelectroelastic moduli for transversely isotropic fibrous composites based on a formalism of Milgrom and Shtrikman.[9] Harshe *et al.*[10] used a cubic model, and Aboudi[11] employed a homogenization micromechanical method to investigate the particulate composites. The classical Eshelby's equivalent inclusion approach and the Mori-Tanaka mean-field model have been generalized to multiferroic composites by Li and Dunn,[12,13] Huang,[14] Li,[15] Wu and Huang,[16] and Srinivas *et al.*[17] The frequency-dependence of the ME coefficients of multiferroic laminates was studied by Bichurin *et al.*[18–20] A complete review of all of this literature can be found in Nan *et al.*[2] and Bichurin *et al.*[19]

Recently, some multi-phase piezoelectric and piezomagnetic composites were made experimentally to enhance the ME coupling. Nan *et al.*[21,22] prepared three-phase ME particulate composites with Terfenol-D particles in a lead zirconate titanate (PZT)-polyvinylidene fluoride (PVDF) mixture, and the measured ME coefficient was enhanced to 45 mV/cm. Gupta and Chatterjee[23] made a three-phase $BaTiO_3$-$CoFe_2O_4$-PVDF particulate composite and showed a maximum ME voltage coefficient around 26 mV/cmOe. Chau *et al.*[24] investigated the ME behavior of composites consisting of Terfenol-D and PZT with the polymer PMMA, polymerized ethylene oxide (PEO), or Li^+-PEO and demonstrated that higher matrix conductivity could enhance the ME signals. Jadhav *et al.*[25] prepared a three-phase combination of $Ni_{0.5}Cu_{0.2}Zn_{0.3}Fe_2O_4/BaTiO_3$/PZT and measured a maximum ME coefficient of 975 μV/cmOe.

The inhomogeneity-coating-matrix composite is a special and interesting three-phase heterogeneous material. The coating, a thin layer of the third phase intervening between an inclusion (or inhomogeneity) and the matrix, creates some important applications. For instance, to reduce the heat or stress concentration along the interface, interphase layers are often introduced to act as thermal barriers. To enhance the electric conductivity of the electric composites, coated fibers are designed to serve as reinforcements. Such coatings may have constant or spatially varying properties.[26] Research into graded multiferroics has primarily been confined to the study

[a)]Author to whom correspondence should be addressed. Electronic mail: hykuo@mail.nctu.edu.tw.

of bilayer and multilayer structures. Among them, piezoelectric or piezomagnetic coefficients are assumed to have linear variation in the direction of the thickness,[27–29] although an exponentially graded assumption was also adopted recently.[30,31] Apart from these laminate structures, Wang and Pan[32] investigated how the imperfect interface affects the ME effect in a multiferroic fibrous composite. Pan *et al.*[33] showed that the nonclassical interface condition exerts a significant influence on the local and overall ME responses, especially when the fibers are at the nanoscale. Wang *et al.*[34] enhanced the ME effect via the curvature of a heterogeneous cylinder. Thostenson *et al.*[35] experimentally coated carbon fibers with carbon nanotubes (CNTs), which were then embedded in a polymer matrix. They showed that CNT-coated carbon fiber composites could improve the local interfacial load transfer, and therefore were likely to reinforce the local strength along the interface of the carbon fiber and the polymer matrix. Good effective thermal conductivity for coated fiber filler composites was also analytically predicted by Hatta and Taya.[36] They theoretically showed that the use of highly conductive or resistive coating, even if its thickness is small, is quite efficient in enhancing the overall thermal conductivity or resistivity. Nicrovici *et al.*[37] studied the equivalence between a coated three-phase composite and the corresponding two-phase composite on the dielectric constants or the transport coefficients.

In this paper, by generalizing Rayleigh's classic approach,[38] we investigate the ME properties of circular fibrous composites under the generalized anti-plane shear deformation. The solution can be for any multicoated circular fibers in a matrix. As a numerical example, we apply our solution to the coated fiber in a matrix made of $BaTiO_3$, $CoFe_2O_4$, and Terfenol-D. This article is organized as follows: We consider, in Sec. II, a composite made of piezoelectric and piezomagnetic phases arranged on a microstructure consisting of parallel cylinders in a matrix. The phases are transversely isotropic and under anti-plane shear with in-plane electromagnetic fields. In this situation, the fields are decoupled in the interior of every phase, and the coupling between the fields occurs only through the interface conditions. We exploit this in detail in Sec. III in order to obtain a representation of the solution for the multicoated circular cylinder. We obtain the effective properties in Sec. IV, and show that the macroscopic (or overall effective) properties depend only on a single expansion coefficient. This methodology is illustrated in Sec. V using composites made of $BaTiO_3$, $CoFe_2O_4$, and Terfenol-D.

II. FORMULATION

Let us consider a composite consisting of a periodic rectangular array of parallel and separated circular cylinders. The domain of the cylinder is denoted by V. We assume that the cylinders and the matrix are made of distinct phases. Further, we assume that each phase is either piezoelectric or piezomagnetic with transversely isotropic symmetry (i.e., has 6*mm* symmetry) about the fiber axis. We introduce a Cartesian coordinate system with the x- and y-axes in the plane of the cross-section and the z-axis along the axes of the cylinders. The origin of the coordinate is positioned at the center O of one of the cylinders (Fig. 1). The sides of the unit cell Ω parallel to the x- and y-axes are, respectively, denoted by α and β, and the cylinders are of the same size.

Let the composite be subjected to anti-plane shear strains $\bar{\varepsilon}_{zx}, \bar{\varepsilon}_{zy}$, in-plane electric fields $\overline{E}_x, \overline{E}_y$, and magnetic fields $\overline{H}_x, \overline{H}_y$ at infinity. Thus the heterogeneous material is in a state of anti-plane shear deformation[8] and can be described by

$$\begin{aligned} u_x = u_y = 0, u_z = w(x,y), \\ \varphi = \varphi(x,y), \psi = \psi(x,y), \end{aligned} \tag{1}$$

where u_x, u_y, and u_z are the elastic displacements along the x-, y-, and z-axes, and φ and ψ are, respectively, the electric and magnetic potentials.

The general constitutive laws for the nonvanishing field quantities can be written in a compact form as

$$\mathbf{\Sigma}_j = \mathbf{L}\mathbf{Z}_j, j = x, y, \tag{2}$$

where

$$\mathbf{\Sigma}_j = \begin{pmatrix} \sigma_{zj} \\ D_j \\ B_j \end{pmatrix}, \mathbf{L} = \begin{pmatrix} C_{44} & e_{15} & q_{15} \\ e_{15} & -\kappa_{11} & -\lambda_{11} \\ q_{15} & -\lambda_{11} & -\mu_{11} \end{pmatrix}, \mathbf{Z}_j = \begin{pmatrix} \varepsilon_{zj} \\ -E_j \\ -H_j \end{pmatrix}. \tag{3}$$

In Eq. (3), σ_{zj}, D_j, B_j, ε_{zj}, E_j, and H_j are the stress, electric displacement, magnetic flux, strain, electric field, and magnetic field, respectively. C_{44}, κ_{11}, μ_{11}, and λ_{11} are the elastic

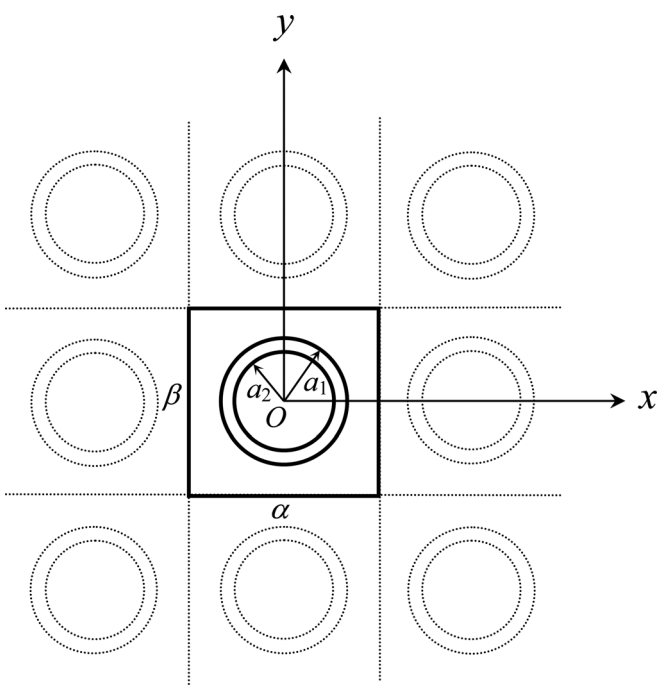

FIG. 1. A schematic representation of the square-arrays composite in which the unit cell is made of a coated cylindrical fiber within the matrix. The volume fraction of the inclusion f, is defined as the ratio of the volume of the fiber plus the coating layer over the total volume of the unit cell (fiber plus coating layer plus matrix). The radius ratio of the fiber over the coating shell is defined as γ.

modulus, dielectric permittivity, magnetic permeability, and ME coefficient, while e_{15} and q_{15} are the piezoelectric and piezomagnetic coefficients. The shear strains ε_{zx} and ε_{zy}, in-plane electric fields E_x and E_y, and in-plane magnetic fields H_x and H_y are related to the gradient of the elastic displacement, electric potential, and magnetic potential.

Making use of the equilibrium equations (in the absence of body force, electric charge density, and electric current density), the elastic displacement w and the electric and magnetic potentials φ and ψ are found to satisfy

$$\begin{aligned} &C_{44}\nabla^2 w + e_{15}\nabla^2\varphi + q_{15}\nabla^2\psi = 0,\\ &e_{15}\nabla^2 w - \kappa_{11}\nabla^2\varphi - \lambda_{11}\nabla^2\psi = 0,\\ &q_{15}\nabla^2 w - \lambda_{11}\nabla^2\varphi - \mu_{11}\nabla^2\psi = 0, \end{aligned} \tag{4}$$

where $\nabla^2 = \partial^2/\partial x^2 + \partial^2/\partial y^2$ represents the two-dimensional Laplace operator for the variables x and y. Because $\mathbf{L}$ is, in general, a nonsingular matrix, we can decouple Eq. (4) into three independent Laplace equations,

$$\nabla^2 w = 0, \nabla^2\varphi = 0, \nabla^2\psi = 0, \tag{5}$$

which should be satisfied in the interior of each phase. In other words, the three fields—elastic displacement, electrostatic potential, and magnetostatic potential—are completely decoupled in the interior of each phase.

These differential equations can be solved, subject to suitable interface and boundary conditions. We assume that the interfaces are perfectly bonded, and therefore the field quantities satisfy

$$\left[\left[\mathbf{\Sigma}_j n_j\right]\right] = \left[\left[\left(\mathbf{L}\mathbf{Z}_j\right)n_j\right]\right] = \mathbf{0}, \left[\left[\mathbf{Z}_j t_j\right]\right] = \mathbf{0}, \tag{6}$$

where $[[\cdot]]$ denotes the jump in the associated quantities across the interface, $\mathbf{n}$ is the unit outward normal to the interface, $\mathbf{t}$ is the unit tangent to the interface, and the repeated index j denotes the summation over the components x and y. Because $\mathbf{L}$ is different in each phase, the fields w, φ, and ψ are generally coupled by the interface equations.

III. MULTICOATED CIRCULAR CYLINDERS

We consider the case in which the fibers are multicoated circular cylinders with an outer radius a_1. We denote the matrix as phase 0, with material parameters $C_{44}{}^{(0)}$, $e_{15}{}^{(0)}$, $q_{15}{}^{(0)}$, $\kappa_{11}{}^{(0)}$, $\mu_{11}{}^{(0)}$, and $\lambda_{11}{}^{(0)}$. The multicoated cylinder consists of a core with radius $r = a_M$, surrounded by $(M-1)$ coating layers. The jth layer of the coatings occupies the annulus $V_j : a_{j+1} \leqq r \leqq a_j, j = 1, 2, ..., M$, in which $V = V_1 \cup V_2 \cup ... \cup V_M$. Because the innermost core is solid, we have $a_{M+1} = 0$. We assume that the material properties of the jth layer of the multicoated cylinder are $C_{44}{}^{(j)}$, $e_{15}{}^{(j)}$, $q_{15}{}^{(j)}$, $\kappa_{11}{}^{(j)}$, $\mu_{11}{}^{(j)}$, and $\lambda_{11}{}^{(j)}$.

Furthermore, without a loss of generality, we consider the situation in which the composite is subjected to a macroscopically uniaxial loading

$$w_{\text{ext}} = \bar{\varepsilon}_{zx}x, \varphi_{\text{ext}} = -\overline{E}_x x, \psi_{\text{ext}} = -\overline{H}_x x \tag{7}$$

for constants $\bar{\varepsilon}_{zx}, \overline{E}_x$, and $\overline{H}_x$. We may write this in short as

$$\Phi_{\text{ext}} = \overline{\mathbf{Z}}_x^{\Phi} x, \tag{8}$$

where Φ represents the appropriate field: the anti-plane deformation w, the electric potential φ, or the magnetic potential ψ.

The potential field (the elastic deformation w, electric potential φ, or magnetic potential ψ) for each layer of the multicoated circular cylinder and its surrounding matrix can be expanded with respect to its center O as[39]

$$\Phi^{(j)}(r,\theta) = A_0^{\Phi(j)} + \sum_{n=1}^{\infty}\left(A_n^{\Phi(j)} r^n + B_n^{\Phi(j)} r^{-n}\right)\cos n\theta \tag{9}$$

for the jth layer, and

$$\Phi^{(0)}(r,\theta) = A_0^{\Phi(0)} + \sum_{n=1}^{\infty}\left(A_n^{\Phi(0)} r^n + B_n^{\Phi(0)} r^{-n}\right)\cos n\theta \tag{10}$$

for the matrix. Here (r,θ) is the polar coordinate centered on the origin of the cylinder. The coefficients $A_n^{\Phi(j)}$ and $B_n^{\Phi(j)}$ are unknowns, to be determined from the interface and boundary conditions. Note that the *sine* terms that would be present in a general expansion are missing because we impose a uniaxial loading along the x-direction only. Further, $\Phi(r,\theta)$ has to be antisymmetric with respect to the y-axis, and thus only terms with an odd number are included. In addition, because the potential at $r \to 0$ should be finite, we can set $B_n^{\Phi(M)} = 0$.

Using the orthogonality properties of trigonometric functions, the interface conditions in Eq. (6) provide

$$\begin{pmatrix} \mathbf{a}_n^{(j-1)} \\ \mathbf{b}_n^{(j-1)} \end{pmatrix} = \mathbf{k}_n^{(j)} \begin{pmatrix} \mathbf{a}_n^{(j)} \\ \mathbf{b}_n^{(j)} \end{pmatrix}, j = 1, 2, ..., M, \tag{11}$$

where

$$\begin{aligned} &\mathbf{a}_n^{(j)} = \begin{pmatrix} A_n^{w(j)} \\ A_n^{\varphi(j)} \\ A_n^{\psi(j)} \end{pmatrix}, \mathbf{b}_n^{(j)} = \begin{pmatrix} B_n^{w(j)} \\ B_n^{\varphi(j)} \\ B_n^{\psi(j)} \end{pmatrix},\\ &\mathbf{k}_n^{(j)} \equiv \begin{pmatrix} \mathbf{I} & a_j^{-2n}\mathbf{I} \\ \mathbf{L}^{(j-1)} & -a_j^{-2n}\mathbf{L}^{(j-1)} \end{pmatrix}^{-1} \begin{pmatrix} \mathbf{I} & a_j^{-2n}\mathbf{I} \\ \mathbf{L}^{(j)} & -a_j^{-2n}\mathbf{L}^{(j)} \end{pmatrix}, \end{aligned} \tag{12}$$

and $\mathbf{I}$ is the 3×3 identity matrix. Now repeated use of Eq. (11) gives

$$\begin{pmatrix} \mathbf{a}_n^{(0)} \\ \mathbf{b}_n^{(0)} \end{pmatrix} = \mathbf{K}_n^{(j)} \begin{pmatrix} \mathbf{a}_n^{(j)} \\ \mathbf{b}_n^{(j)} \end{pmatrix}, j = 1, 2, ..., M, \tag{13}$$

with

$$\mathbf{K}_n^{(j)} \equiv \mathbf{k}_n^{(1)}\mathbf{k}_n^{(2)} \cdots \mathbf{k}_n^{(j)}. \tag{14}$$

For $j = M$, we have

$$\begin{pmatrix} \mathbf{a}_n^{(0)} \\ \mathbf{b}_n^{(0)} \end{pmatrix} = \mathbf{K}_n^{(M)} \begin{pmatrix} \mathbf{a}_n^{(M)} \\ \mathbf{b}_n^{(M)} \end{pmatrix}. \tag{15}$$

Furthermore, according to Eq. (15), and keeping in mind that $B_n^{\Phi(M)} = 0$, we have

$$\mathbf{a}_n^{(0)} = \left[\mathbf{K}_n^{(M)}\right]_{11}\left[\mathbf{K}_n^{(M)}\right]_{21}^{-1}\mathbf{b}_n^{(0)}, \tag{16}$$

where $[\mathbf{K}_n{}^{(M)}]_{11}$ and $[\mathbf{K}_n{}^{(M)}]_{21}$ are, respectively, the upper-left and lower-left (3×3) submatrices of $\mathbf{K}_n{}^{(M)}$.

Finally, imposing the periodicity conditions yields a generalized Rayleigh's identity,[39]

$$A_n^{\Phi(0)} + \sum_{m=1}^{\infty} S_{m+n} B_m^{\Phi(0)} = \overline{Z}_x^{\Phi}\delta_{n,1}, \tag{17}$$

with

$$S_m = \sum_{l\neq o} \mathrm{Re}(X_l + iY_l)^{-m} \tag{18}$$

being the lattice sums characterizing the geometry of the periodic structure, and $(X_l + iY_l)$ the center of the lth cylinder when measured at the central point O. The index l runs over all the cylinders underlying the periodic array except for the central one. A list of nonzero normalized lattices for square arrays can be found in Berman and Greengard.[40]

Equations (16) and (17) constitute an infinite set of linear algebraic equations. Upon appropriate truncation of the expansion terms, we can determine the expansion coefficients $A_n^{\Phi(j)}$ and $B_n^{\Phi(j)}$. Once these coefficients are obtained, we have the solutions for the elastic deformation w, electric potential φ, or magnetic potential ψ. By taking the derivatives, we can finally obtain the field solutions in each phase of the composite.

IV. EFFECTIVE MODULI

Our solutions above are now applied to derive the effective properties. Here we concentrate on a square array, i.e., $\alpha = \beta$. Although in the case of elasticity a square arrangement of circular cylinders results, in general, in a square symmetry,[41] it turns out that in the case of conduction, square symmetry and transverse isotropy become identical.[42] This statement is also correct for magnetoelectricity under the generalized anti-plane shear deformation, which is the case in our study. Therefore, there is no distinction between the effective properties of the x- and y-axes.

We first recall the basic definition of the effective magnetoelectroelastic parameter $\mathbf{L}^*$, given by

$$\langle \mathbf{\Sigma}_j \rangle = \mathbf{L}^* \langle \mathbf{Z}_j \rangle, \tag{19}$$

where the angular brackets denote the area averages over the unit cell Ω, i.e.,

$$\langle \mathbf{\Sigma}_j \rangle = \frac{1}{\Omega}\int_{\Omega} \mathbf{\Sigma}_j dv, \langle \mathbf{Z}_j \rangle = \frac{1}{\Omega}\int_{\Omega} \mathbf{Z}_j dv. \tag{20}$$

For the given far-field in Eq. (7), we can compute the average $\mathbf{Z}_x$ by noting that each component is a gradient and applying the divergence theorem. We obtain

$$\langle Z_x^{\Phi} \rangle = \overline{Z}_x^{\Phi}. \tag{21}$$

Next, in order to find $\langle \Sigma_x^{\Phi} \rangle$, we again use the divergence theorem, equilibrium condition, and interface conditions to arrive at

$$\begin{aligned}\langle \Sigma_x^{\Phi} \rangle &= \frac{1}{\Omega}\int_{\Omega} \Sigma_x^{\Phi} dv = \frac{1}{\Omega}\int_{\Omega} \nabla\cdot\left(x\mathbf{\Sigma}^{\Phi}\right) dv \\ &= \frac{1}{\Omega}\int_{\partial\Omega} x\left(\mathbf{\Sigma}^{\Phi}\right)_m \cdot \mathbf{n} ds,\end{aligned} \tag{22}$$

where

$$\mathbf{\Sigma}^w = \left(\varepsilon_{zx}, \varepsilon_{zy}\right), \mathbf{\Sigma}^{\varphi} = \left(D_x, D_y\right), \mathbf{\Sigma}^{\psi} = \left(B_x, B_y\right). \tag{23}$$

We then use field expansions (9) and (10) to obtain

$$\frac{1}{\Omega}\int_{\partial\Omega} x\left(\mathbf{Z}^{\Phi}\right)_m \cdot \mathbf{n} ds = \overline{Z}_x^{\Phi} - \frac{2\pi B_1^{\Phi(0)}}{\alpha\beta}. \tag{24}$$

Here

$$\mathbf{Z}^w = \left(\varepsilon_{zx}, \varepsilon_{zy}\right), \mathbf{Z}^{\varphi} = -\left(E_x, E_y\right), \mathbf{Z}^{\psi} = -\left(H_x, H_y\right). \tag{25}$$

Putting Eqs. (22) and (24) together, and recalling the constitutive relation (2) for the matrix, we obtain

$$\begin{pmatrix} \langle \sigma_{zx} \rangle \\ \langle D_x \rangle \\ \langle B_x \rangle \end{pmatrix} = \begin{pmatrix} C_{44} & e_{15} & q_{15} \\ e_{15} & -\kappa_{11} & -\lambda_{11} \\ q_{15} & -\lambda_{11} & -\mu_{11} \end{pmatrix}^{(0)} \begin{pmatrix} \overline{\varepsilon}_{zx} - \frac{2\pi B_1^{w(0)}}{\alpha\beta} \\ -\overline{E}_x - \frac{2\pi B_1^{\varphi(0)}}{\alpha\beta} \\ -\overline{H}_x - \frac{2\pi B_1^{\psi(0)}}{\alpha\beta} \end{pmatrix}. \tag{26}$$

Putting together Eqs. (19) and (26), and noting that the coefficient $B_1^{\Phi(0)}$ depends linearly on the applied field, we obtain the equations for the effective property $\mathbf{L}^*$.

V. RESULTS AND DISCUSSION

As a numerical example, we apply our solution to a single coated fiber, i.e., $M = 2$, for which the radii of the (fiber) core and coating shell are, respectively, a_2 and a_1. For the piezoelectric material, we consider the widely used $BaTiO_3$ (BTO). For the piezomagnetic material we consider $CoFe_2O_4$ (CFO) as well as the Terfenol-D alloy (TD). All of these are transversely isotropic. The material properties are listed in Table I in Voigt notation, where the *xoy* plane is isotropic

TABLE I. Material parameters of $BaTiO_3$, $CoFe_2O_4$ (Ref. 12), and Terfenol-D (Refs. 43 and 44).

Property	$BaTiO_3$	$CoFe_2O_4$	Terfenol-D
C_{44} (N/m^2)	43×10^9	45.3×10^9	13.6×10^9
e_{15} (C/m^2)	11.6	0	0
q_{15} (N/Am)	0	550	108.3
κ_{11} (C^2/Nm^2)	11.2×10^{-9}	0.08×10^{-9}	0.05×10^{-9}
μ_{11} (Ns^2/C^2)	5×10^{-6}	590×10^{-6}	5.4×10^{-6}
λ_{11} (Ns/VC)	0	0	0

and the unique axis is along the z-direction. Note that in all materials the ME coefficients are zero, i.e., $\lambda_{11} = 0$.

The ratio of the radius between the circular fiber and the coating shell is defined as $\gamma = a_2/a_1$, and the coated fibers are embedded in the matrix in a square array pattern. It is obvious that if $\gamma = 0$, then $a_2 = 0$. In other words, there is no fiber phase. On the other hand, if $\gamma = 1$, it means that there is no coating shell. In our study, we are particularly interested in the ME voltage coefficient, which is the important figure of merit for magnetic field sensors. It relates the overall electric field that is generated in the composite when it is subjected to a magnetic field. It combines the coupling and dielectric coefficients, and is defined by

$$\alpha_{11}^* = \lambda_{11}^*/\kappa_{11}^*. \tag{27}$$

Figure 2 shows the dependence of the ME coefficient in coated fibrous composites on both the volume fraction f and the ratio of the radii of the fiber and the shell $\gamma = a_2/a_1$. The volume fraction is defined as the volume of the fiber and the coated shell over the total volume (i.e., the fiber, plus the coated shell and the matrix). Figure 2(a) is for (fiber/coating/matrix) = (BTO/TD/CFO). It is observed that, for a fixed volume fraction, the ME effect increases when the radii's ratio γ increases from 0 to 0.70; then it decreases with increasing γ. Furthermore, for a fixed γ, the ME effect increases with increasing volume fraction and, in most cases, reaches its maximum where the volume fraction f is around 0.74. Figure 2(b) shows the corresponding results when the fiber and coating shell in Fig. 2(a) are switched. Compared to Fig. 2(a), it is obvious that although the magnitude of the ME is about the same, the direction or the sign has been changed. Furthermore, the maximum magnitudes are all reached around $f = 0.30$, and the magnitude increases with increasing γ from 0 to 0.94 (the maximum ME effect is about 0.740 V/cmOe, slightly larger than in the first case).

Figure 2(c) shows the ME effect for the composite made of (fiber/coating/matrix) = (BTO/CFO/TD). The ME effect is positive, and for fixed f, it increases with increasing γ (from 0 to 0.84). It reaches its maximum value 3.304 V/cm Oe at $\gamma = 0.84$, and then it decreases. Furthermore, for any fixed γ, the ME effect reaches its maximum when f is around 0.70. Figure 2(d) shows the ME effect in the composite when the coating shell and fiber in Fig. 2(c) are switched.

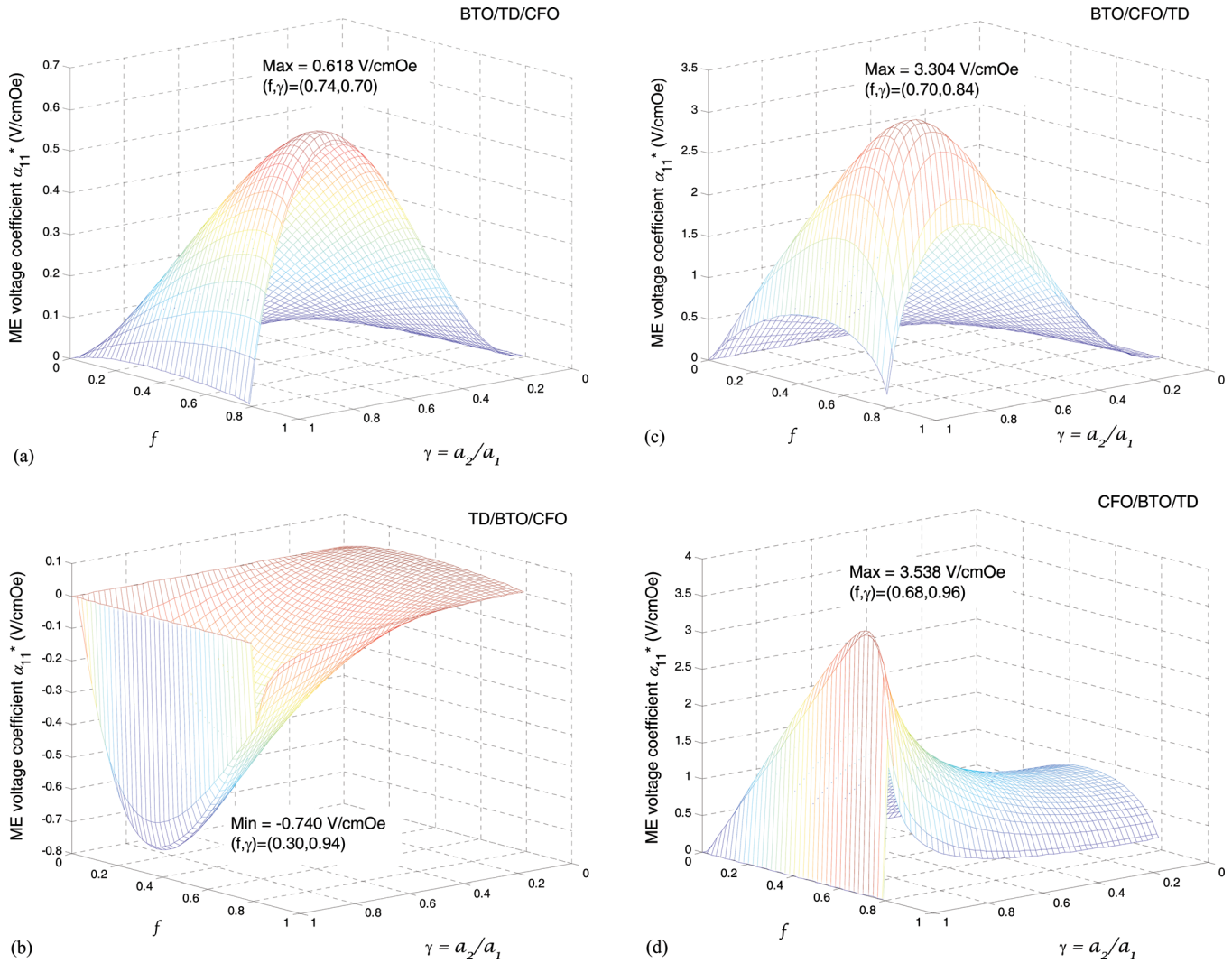

FIG. 2. (Color online) The effective ME voltage coefficient α_{11}^* vs the volume fraction of the inclusion f and the radius ratio γ. The composite is in a square array where coated cylindrical fibers are embedded in the matrix. (a) BTO fiber coated by TD, with both in a CFO matrix. (b) TD fiber coated by BTO, with both in a CFO matrix. (c) BTO fiber coated by CFO, with both in a TD matrix. (d) CFO fiber coated by BTO, with both in a TD matrix.

Similarly, the ME effect increases from $\gamma = 0$ to 0.96, and then decreases. Also, in Figs. 2(c) and 2(d), the maximum ME value is about 3.5 V/cmOe, and in Figs. 2(a) and 2(b) it is only about 0.7 V/cmOe. Furthermore, as compared to the uncoated case, where the ME value is either zero or very small, the ME effect in the coated fibrous composites can be enhanced by 10 times. Similar trends are also observed if we replace BTO with PZT-5A.

VI. CONCLUSIONS

We have extended Rayleigh's formalism on periodic conductive composites to a magnetoelectroelastic composite consisting of multicoated circular cylinders under anti-plane shear deformation, in-plane electric field, and in-plane magnetic intensities. Expressions for the effective moduli of the composite are derived. As a practical example, explicit numerical calculations for the ME effects of a BTO/CFO/TD coated composite are presented and discussed. These examples show that with a coating appropriate for the inhomogeneity (fiber), the effective ME effect can be enhanced by one order of magnitude as compared to the noncoated counterpart. While our numerical results are based on piezoelectric $BaTiO_3$ and piezomagnetic $CoFe_2O_4$ or Terfenol-D, the enhancement of the ME effect based on other materials, such as $BiFeO_3$, $NiFe_2O_4$, etc., could be possible. Therefore, different material phases and volume fraction ratios are some alterative channels for improving the effective material properties of multiferroic composites.

ACKNOWLEDGMENTS

We are glad to acknowledge financial support from the National Science Council, Taiwan, under Grant No. NSC 99-2221-E-009-053 and from a special program in Henan Province.

[1]W. Eerenstein, N. D. Mathur, and J. F. Scott, Nature **442**, 759 (2006).
[2]C.-W. Nan, M. I. Bichurin, S. Dong, D. Vieland, and G. Srinivasan, J. Appl. Phys. **103**, 031101 (2008).
[3]T. R. McGuire, E. J. Scott, and F. H. Grannis, Phys. Rev. **102**, 1000 (1956).
[4]N. A. Spaldin and M. Fiebig, Science **309**, 391 (2005).
[5]G. Srinivasan, Annu. Rev. Mater. Res. **40**, 153 (2010).
[6]C.-W. Nan, Phys. Rev. B **50**, 6082 (1994).
[7]J. H. Huang, and W.-S. Kuo, J. Appl. Phys. **81**, 378 (1997).
[8]Y. Benveniste, Phys. Rev. B **51**, 16424 (1995).
[9]M. Milgrom, and S. Shtrikman, Phys. Rev. A **40**, 1568 (1989).
[10]G. Harshe, J. P. Dougherty, and R. E. Newnham, Int. J. Appl. Electromagn. Mater. **4**, 161 (1993).
[11]J. Aboudi, Smart Mater. Struct. **10**, 867 (2001).
[12]J. Y. Li and M. L. Dunn, J. Intell. Mater. Syst. Struct. **9**, 404 (1998).
[13]J. Y. Li and M. L. Dunn, Philos. Mag. A **77**, 1341 (1998).
[14]J. H. Huang, Phys. Rev. B **58**, 12 (1998).
[15]J. Y. Li, Int. J. Eng. Sci. **38**, 1993 (2000).
[16]T. L. Wu and J. H. Huang, Int. J. Solids Struct. **37**, 2981 (2000).
[17]S. Srinivas, J. Y. Li, Y. C. Zhou, and S. K. Soh, J. Appl. Phys. **99**, 043905 (2006).
[18]M. I. Bichurin, V. M. Petrov, and G. Srinivasan, Phys. Rev. B **68**, 054402 (2003).
[19]M. I. Bichurin, V. M. Petrov, S. V. Averkin, and E. Liverts, J. Appl. Phys. **107**, 053904 (2010).
[20]M. I. Bichurin, V. M. Petrov, S. V. Averkin, and E. Liverts, J. Appl. Phys. **107**, 053905 (2010).
[21]C.-W. Nan, L. Lu, N. Cai, J. Zhai, Y. Ye, Y. H. Lin, L. J. Dong, and C. X. Xiong, Appl. Phys. Lett. **81**, 3831 (2002).
[22]C.-W. Nan, N. Cai, L. Liu, J. Zhai, Y. Ye, and Y. Lin, J. Appl. Phys. **94**, 5930 (2003).
[23]A. Gupta and R. Chatterjee, J. Appl. Phys. **106**, 024110 (2009).
[24]K. H. Chau, Y. W. Wong, and F. G. Shin, Appl. Phys. Lett. **94**, 202902 (2009).
[25]P. A. Jadhav, M. B. Shelar, and B. K. Chougule, J. Alloy Compd. **479**, 385 (2009).
[26]S. Suresh, Science **292**, 2447 (2001).
[27]W. Q. Chen and K. Y. Lee, Int. J. Solids Struct. **40**, 5689 (2003).
[28]V. M. Petrov and G. Srinivasan, Phys. Rev. B **78**, 184421 (2008).
[29]V. M. Petrov, G. Srinivasan, and T. A. Galkina, J. Appl. Phys. **104**, 113910 (2008).
[30]E. Pan and F. Han, Int. J. Eng. Sci. **43**, 321 (2005).
[31]X. Wang, E. Pan, J. D. Albrecht, and W. J. Feng, Compos. Struct. **87**, 206 (2009).
[32]X. Wang and E. Pan, Phys. Rev. B **76**, 214107 (2007).
[33]E. Pan, X. Wang, and R. Wang, Appl. Phys. Lett. **95**, 181904 (2009).
[34]H. M. Wang, E. Pan, and W. Q. Chen, J. Appl. Phys. **107**, 093514 (2010).
[35]E. T. Thostenson, W. Z. Li, D. Z. Wang, and Z. F. Ren, J. Appl. Phys. **91**, 6034 (2002).
[36]H. Hatta and M. Taya, J. Appl. Phys. **59**, 1851 (1986).
[37]N. A. Nicrovici, R. C. McPhedran, and G. W. Milton, Proc. R. Soc. London, Ser. A **442**, 599 (1993).
[38]L. Rayleigh, Philos. Mag. **34**, 481 (1892).
[39]H.-Y. Kuo and K. Bhattacharya, Mech. Mater. (under revision).
[40]C. L. Berman and L. Greengard, J. Math. Phys. **35**, 6036 (1994).
[41]S. Li, Composites, Part A **32**, 815 (2000).
[42]D. R. Perrins, D. R. McKenzie, and R. C. McPhedran, Proc. R. Soc. London, Ser. A **369**, 207 (1979).
[43]Y. X. Liu, J. G. Wan, J.-M. Liu, and C. W. Wen, J. Appl. Phys. **94**, 5111 (2003).
[44]G. Liu, C.-W. Nan, N. Cai, and Y. Lin, J. Appl. Phys. **95**, 2660 (2004).